Article

Journal of
Nanoscience and Nanotechnology
Vol. 19, 1056–1060, 2019
www.aspbs.com/jnn

Highly Efficient Blue Organic Light-Emitting Diodes Based on Diarylamine-Substituted Pyrene Derivatives

Seokwon Cho[1], Namhee Hwang[1], Song Eun Lee[2], Young Kwan Kim[2,*], and Seung Soo Yoon[1,*]

[1] *Department of Chemistry, Sungkyunkwan University, Suwon, Kyeonggi-do 440-746, Korea*
[2] *Department of Information Display, Hongik University, Seoul, 121-791, Korea*

In this study, we designed and synthesized three blue fluorescence materials based on diarylamine-substituted pyrene derivatives. Organic Light Emitting-Diodes devices using these materials were fabricated in the following sequence; ITO/2-TNATA (300 Å)/NPB (200 Å)/α,β-ADN: 10 wt% blue materials **1–3** (300 Å)/DNAB (300 Å)/Liq (20 Å)/Al (1000 Å). All devices showed highly efficient blue emissions. Particularly, a device using materials (**3**) shown highly efficient blue emission with luminous efficiency of 8.94 cd/A, power efficiency of 4.40 lm/W, external quantum efficiency of 6.62% at 20 mA/cm^2, respectively, and the CIE coordinates of (0.16, 0.23) at 6.0 V.

Keywords: Blue OLED, Fluorescence, Pyrene, Arylamine.

1. INTRODUCTION

In recent display market, organic light-emitting diodes (OLEDs) are received intensive attention because of their potential application to next generation display such as flexible and transparent displays.[1,2] However, there are still problems, among which is the lifetime of the blue light emitting material.[3] This problem on blue-emitting materials is caused by intrinsic instability and wide band-gap energy of molecules.[4] Until recently, a lot of researches have been continuing to overcome these problems. In particular, pyrene, anthracene, chrysene, and phenanthrene derivatives have been reported by many groups because these materials have important properties for blue emitting materials of OLED such as wide energy gap, high fluorescence quantum yield and high thermal stability.[5–7] For example, Wang et al. synthesized 1,6-bis(3,5-diphenylphenyl)pyrene that exhibited a luminous efficiency (LE) and a CIE coordinate of 3.26 cd/A and (0.15, 0.11) at 6.0 V.[8] Also, Jeong et al. synthesized a pyrene derivative containing two carbazole moieties at 1,6-position of pyrene with the maximum emission wavelength of 488 nm and the LE of 3.67 cd/A.[9] Moreover, Chercka et al. reported a material that introduced phenyl carbazole at positions 2 and 7 of pyrene with CIE coordinate of (0.16, 0.24) and a maximum external quantum efficiency (EQE) of 3.19%.[10]

Herein, we newly designed and synthesized blue fluorescence materials based on diarylamine-substituted three pyrene derivatives (material **1**, **2**, and **3**) for OLEDs. To suppress the self-aggregation effect that reduces electroluminescence (EL) efficiencies, two bulky diarylamine groups were introduced at positions of 1 and 6 of pyrene. This structural property effectively prevent red-shifted emission caused by intermolecular interaction in solid state, which lead to high color purity of EL emission.[11] Also, for effective blue emission, we introduced electron withdrawing moiety (nitrile) at *para*-position of linkage, which would lead to lower the highest occupied molecular orbital (HOMO) energy level of the molecules and make it have the appropriate band-gap energy for blue emission.[12] Moreover, diarylamine moiety would improve their hole transporting abilities and enhance charge balance in the emitting-layer (EML).[13] Therefore, OLED device using these properties of materials **1–3** would lead to the highly efficient blue emission.

2. EXPERIMENTAL DETAILS

2.1. Synthesis

2.1.1. 4,4′-[1,6-Pyrenediylbis(phenylamino)]bis-Benzonitrile (1)

Material **1** was prepared by the following Buchwald-Hartwig reaction procedure using 1,6-dibromopyrene (1.39 mmol), 4-(phenylamino)benzonitrile (3.06 mmol),

---

[*] Authors to whom correspondence should be addressed.

1533-4880/2019/19/1056/005 doi:10.1166/jnn.2019.15929

Tris(dibezylideneacetone)dipalladium(0) (0.069 mmol), 2-Dicyclohexylphosphino-2′,6′-dimethoxybiphenyl (0.11 mmol), sodium *tert*-butoxide (9.72 mmol) (Yield: 40.5%). ^{1}H-NMR (500 MHz, $CDCl_3$) [δ ppm]; 8.20 (d, $J = 8.15$ Hz, 2H), 8.10 (d, $J = 9.18$ Hz, 2H), 8.02 (d, $J = 9.25$ Hz, 2H), 7.87 (d, $J = 8.10$ Hz, 2H), 7.42 (d, $J = 8.92$ Hz, 4H), 7.34 (t, $J = 7.38$ Hz, 4H), 7.26 (d, $J = 8.43$ Hz, 4H), 7.16 (t, $J = 7.32$ Hz, 2H), 6.90 (d, $J = 8.91$ Hz, 4H); APCI-MS $m/z = 586[M^+]$; Anal. Calcd for $C_{42}H_{26}N_4$: C, 85.98; H, 4.47; N, 9.55. Found: C, 85.23; H, 4.15; N, 8.97.

2.1.2. 4,4′-[1,6-Pyrenediylbis((3,5-diphenyl)phenylamino)]bis-Benzonitrile (2)

The synthetic procedure for material **2** was similar to that described for material **1** using 4-((1,3-diphenyl)phenylamino)benzonitrile (3.06 mmol) instead of 4-(phenylamino)benzonitrile, the desired compound was obtained as a yellow solid (Yield: 51.3%). ^{1}H-NMR (500 MHz, $CDCl_3$) [δ ppm]; 8.22 (d, $J = 8.15$ Hz, 2H), 8.11 (d, $J = 9.18$ Hz, 2H), 8.01 (d, $J = 9.25$ Hz, 2H), 7.86 (d, $J = 8.10$ Hz, 2H), 7.55 (m, 8H), 7.41 (d, $J = 8.92$ Hz, 4H), 7.33 (m, 12H), 7.28 (d, $J = 8.43$ Hz, 4H), 7.10 (s, 2H), 6.95 (s, 2H); APCI-MS $m/z = 890[M^+]$; Anal. Calcd for $C_{66}H_{42}N_4$: C, 88.96; H, 4.75; N, 6.29. Found: C, 88.35; H, 4.47; N, 6.11.

2.1.3. 4,4′-[1,6-Pyrenediylbis(9,10-dimethylfluoren-2-yl-amino)]bis-Benzonitrile (3)

The synthetic procedure for material **3** was similar to that described for 1 using 4-(9,10-dimethylfluoren-2-yl-amino)benzonitrile (3.06 mmol) instead of 4-(phenylamino)benzonitrile, the desired compound was obtained as a yellow solid (Yield: 37.5%). ^{1}H-NMR (500 MHz, $CDCl_3$) [δ ppm]; 8.19 (d, $J = 8.15$ Hz, 2H), 8.12 (d, $J = 9.18$ Hz, 2H), 8.03 (d, $J = 9.25$ Hz, 2H), 7.82 (d, $J = 8.10$ Hz, 2H), 7.54 (m, 6H), 7.40 (d, $J = 8.92$ Hz, 4H), 7.33 (m, 4H), 7.28 (d, $J = 8.43$ Hz, 4H), 7.12 (d, $J = 8.53$ Hz, 2H), 6.93 (s, 2H), 0.51 (s, 12H); APCI-MS $m/z = 818[M^+]$; Anal. Calcd for $C_{60}H_{42}N_4$: C,87.99; H, 5.17; N, 6.84. Found: C, 87.32; H, 4.95; N, 6.51.

2.2. OLED Fabrication and Measurements

For OLED fabrication, indium-tin-oxide (ITO) thin films coated on glass substrates were used, which were 30 Ω/square of the sheet resistively and 1000 Å thick. The ITO-coated glass was cleaned in an ultrasonic bath through the following sequence: washes with acetone, methyl alcohol, and distilled water, storage in isopropyl alcohol for 48 h, and drying with a N_2 gas gun.

The substrates were treated by O_2 plasma under 2×10^{-2} Torr at 125 W for 2 min. All organic materials and metal were deposited under high vacuum (5×10^{-7} Torr). The current density (J), luminance (L), luminous efficiency (LE), and CIE chromaticity coordinates of the OLEDs were measured with a Keithly 2400, Chroma meter CS-1000A. Electroluminance was measured using a Roper Scientific Pro 300i.

3. RESULTS AND DISCUSSION

Syntheses of three blue fluorescent materials **1–3** are shown in Scheme 1.

Density functional theory (DFT) calculations for blue fluorescent materials **1–3** using the Becke's three parameterized Lee-Yang-Parr (B3LYP) functional with 6-31G* basis sets using a suite of Gaussian programs were carried out to understand the observed properties of the materials **1–3** on molecular levels. The electron cloud distributions of LUMO in materials **1–3** are mainly located in pyrene moiety which is center of molecules. In material **1** and **3**, the electron cloud distributions of HOMO are spread widely throughout the molecules. And the electron cloud distributions of HOMO in material **2** are located in throughout the molecule apart from two phenyl rings introduced into diarylamine.

As shown in Figure 1, three-dimensional structures of materials **1–3** demonstrated that molecules have twisted structure because of introducing of diarylamine moieties at 1,6-positions of pyrene. The dihedral angles between pyrene and benzonitrile moiety substituted at the 1,6-position of pyrene were calculated to be 56°, 57°, and 67° for materials **1**, **2**, and **3**, respectively. Also, the dihedral angles between pyrene and other aromatic ring moieties (benzene, diphenylbenzene, fluorene) were calculated to be 67°, 69°, and 35° for materials **1**, **2**, and **3**, respectively. These twisted structural features of materials would effectively suppress the aggregation-quenching by π–π stacking in solid state, which is leading to electroluminescent (EL) efficiency.[14]

The UV-Visible absorption spectra of materials **1–3** and emission spectrum of α, β-ADN in dilute dichloromethane solution are shown in Figure 2(a). And the photoluminescence (PL) spectra of materials **1–3** in dilute solution Figure 2(b). Their photophysical properties are summarized in Table I. In Figure 2(a), the maximum absorption wavelength (λ_{max}) of materials **1–3** appeared at 243 nm, 247 nm and 270 nm in dilute dichloro methane solution (1×10^{-5} M), respectively. Also, all materials (**1–3**) exhibited strong absorption peaks near 330 nm and 405 nm. And the maximum emission wavelength of materials **1–3** occurred at 459, 458 and 476 nm in dichloromethane solution (1×10^{-5} M), respectively, in blue region of the visible spectrum. The maximum intensity of PL spectra of material **3** showed more red-shifted than material **1** and **2**.

The conjugation length of the aryl group in material **3** is longer than other materials (**1** and **2**), which is leading to red-shifted emission.[15]

To investigate the EL properties of materials **1–3**, OLED devices **A–C** were fabricated as

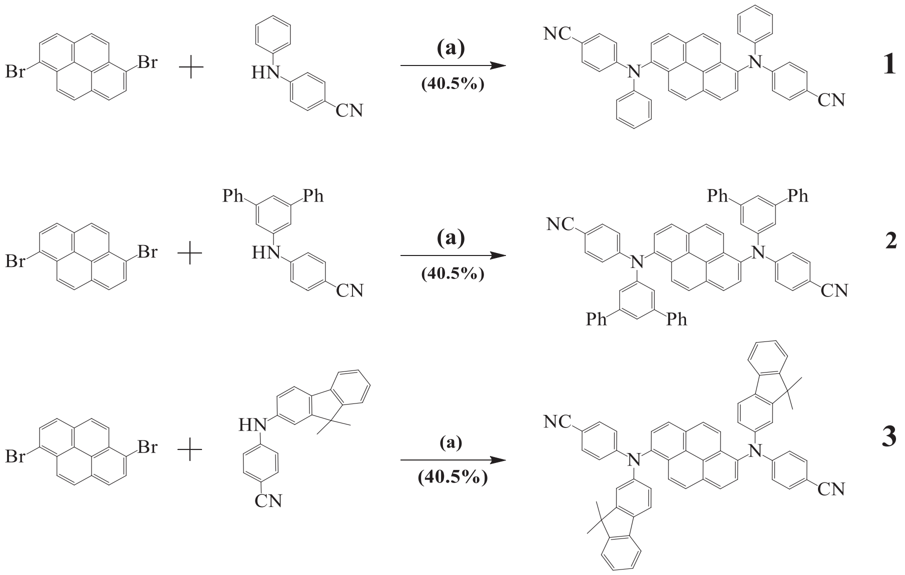

Scheme 1. Synthesis of materials 1–3; (a) $Pd_2(dba)_3$, toluene, sphos, NaO-tBu, reflux.

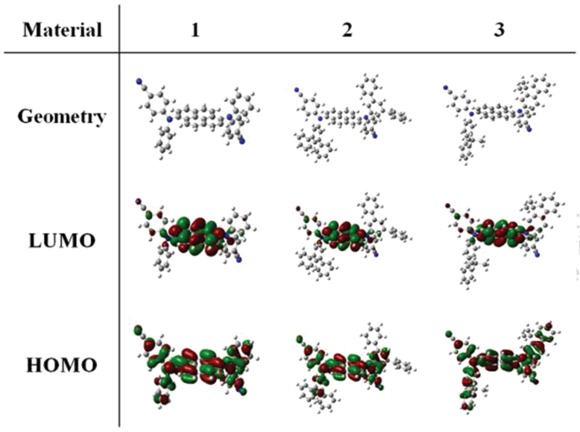

Figure 1. Density functional theory (DFT) calculations for blue fluorescent materials 1–3.

Table I. Physical properties of materials 1–3.

Material	UV λ^a_{max} (nm)	PL λ^a_{max} (nm)	FWHM^a (nm)	HOMO/LUMO^b (eV)	E^c_g (eV)	Φ^d_f
1	243	452	44	−5.34/−2.44	2.90	0.64
2	247	453	43	−5.33/−2.41	2.92	0.61
3	241	476	61	−5.03/−2.23	2.80	0.75

Notes: ^{a}Measured in CH_2Cl_2 (ca. 1×10^{-5} M). ^{b}HOMO energy level was determined by low-energy photoelectron spectrometer and LUMO = HOMO + E_g. ^{c}Determined from the intersection of the absorption and photoluminescence spectra. ^{d}PL quantum yields were determined in CH_2Cl_2 solution at 298 K against 9,10-diphenylanthracene (DPA) as a reference; λ_{ex} = 360 nm (Φ = 0.90 in CH_2Cl_2 solution).

following structure: ITO (180 nm)/4,4′,4″-Tris[2-naphthyl(phenyl)amino]triphenylamine (2-TNATA) (300 nm)/ *N*,*N*′-diphenyl-*N*,*N*′-(2-napthyl)-(1,1′-phenyl)-4,4′-diamine (NPB) 200 nm/10-(1-naphthalenyl)-9-(2-naphthalenyl) anthracene (α, β-ADN): 10 wt% blue materials **1–3** (300 nm)/2-(4-(9,10-di(naphthalen-2-yl)anthracen-7-yl) phenyl)-1-phenyl-1H-benzo[*d*]imidazole (DNAB) (300 nm)/ lithium quinolate (Liq) (20 nm)/Al (1000 nm). 2-TNATA and NPB were selected as the hole injection layer (HIL) and hole transporting layer (HTL), respectively. Materials **1–3** were used blue dopants in emitting layer (EML), α, β-ADN was selected host material in EML, and DNAB

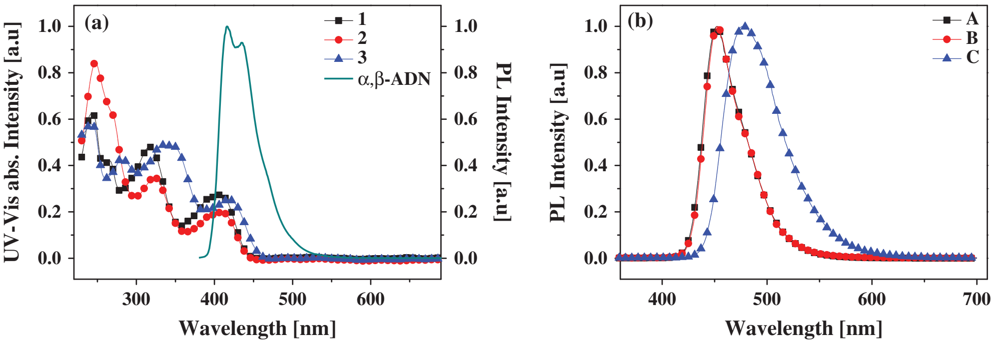

Figure 2. (a) UV-visible absorption spectra of materials 1–3 and PL emission spectra of α,β-ADN; (b) PL emission spectra of materials 1–3 in 10^{-5} M CH_2Cl_2 solution.

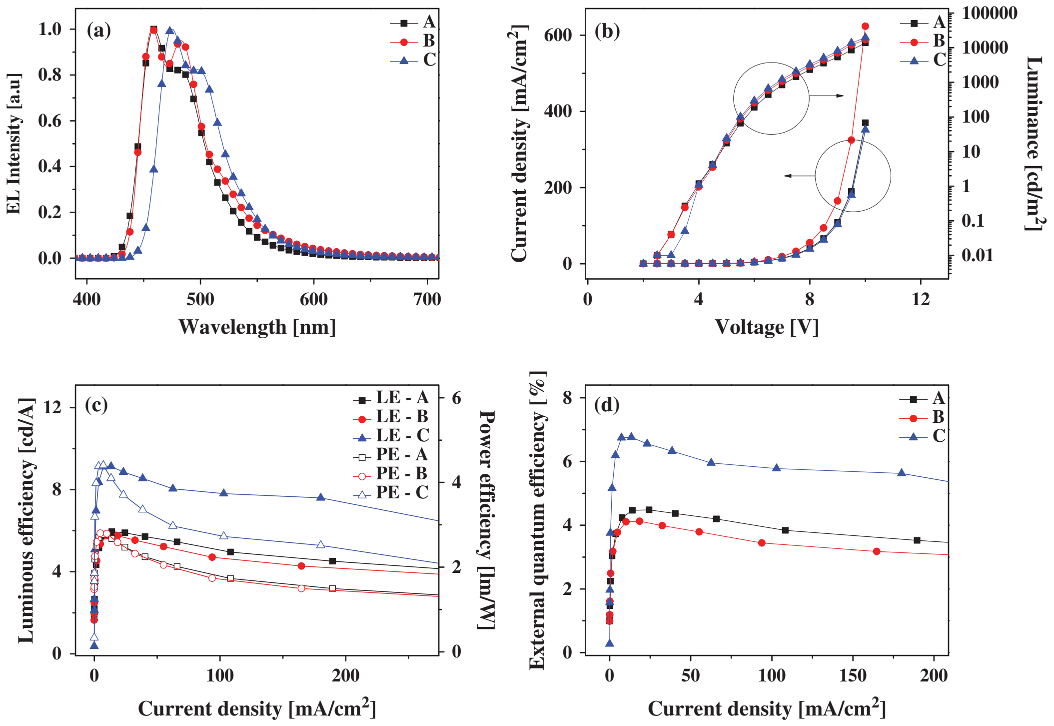

Figure 3. (a) EL spectra of devices A–C; (b) current density–voltage–luminance (*J*–*V*–*L*) characteristics of devices A–C; (c) luminous efficiency and power efficiency of devices A–C; (d) external quantum efficiency of devices A–C.

was chosen as the electron-transporting layer (ETL). ITO and Liq on the Al were selected anode and cathode, respectively.

Figure 3(a) shows the EL spectra of device **A–C**, and their EL properties are summarized in Table II. Maximum intensity of device **A–B** occurred 459, 458, and 475 nm in blue region, respectively. Maximum EL emission peak of all devices matched PL maximum peaks of materials **1–3** in dichloromethane solution. These results indicate that EL emissions of all devices were from the singlet excition of blue dopant materials **1–3**. On the other hand, they demonstrated a large shoulder peak with red-shifted due to excimer formation in high doping concentration of solid state.[16] The Commission International de L'Eclairage (CIE) chromaticity coordinates of devices **A–C** were (0.14, 0.17), (0.15, 0.18), and (0.16, 0.23) at 6.0 V, respectively.

Figures 3(b)–(d) demonstrate the current density-voltage-luminance (*J*–*V*–*L*) characteristics, luminous efficiencies, power efficiencies and external quantum efficiencies of devices **A–C**. Devices **A–C** were exhibited highly efficient blue emissions with the luminous efficiencies of 5.16, 5.35 and 8.94 cd/A, power efficiencies of 2.70, 2.80, and 3.84 lm/W, and external quantum efficiencies of 3.72, 3.78, and 6.62% at 20 mA/cm², respectively. And maximum values of the external quantum efficiencies of devices **A–C** were 4.47, 4.12, and 6.76%, respectively. Interestingly, device **C** using material **3** showed the more efficient EL efficiencies than other devices. Compared to material **1** and **2** ($\Phi_f = 0.64$, 0.61, respectively), material **3** ($\Phi_f = 0.75$) has the better fluorescence quantum yield in dilute solution. Furthermore, as shown in Figure 2(a), the overlap of the emission spectrum of α, β-AND host with the absorption spectrum of dopant **3** is larger than those of dopants **1** and **2**. These observations imply that the Föster energy transfer from host to dopant in device **C** is more effective than those in devices **A** and **B**, and thus lead to the improved EL efficiencies of device **C** in comparison with devices **A** and **B**.

Table II. EL properties of devices A–C.

Device	Material^a	EL $\lambda^b_{\max}$ (nm)	L^c (cd/m²)	LE$^{c/d}$ (cd/A)	PE$^{c/d}$ (lm/W)	EQE$^{c/d}$ (%)	CIE^b (x, y)
A	1	459	13,820	5.95/5.16	2.77/2.70	4.47/3.72	(0.14, 0.17)
B	2	458	17,110	5.77/5.35	2.80/2.80	4.12/3.78	(0.15, 0.18)
C	3	475	19,505	9.13/8.94	4.40/3.84	6.76/6.62	(0.16, 0.23)

Notes: ^{a}Doping concentration (10% weight). ^{b}At 6.0 V. ^{c}Maximum values. ^{d}Measured at a current density of 20 mA/cm².

4. CONCLUSION

We synthesized three pyrene derivatives endcapped with diarylamine moieties. Blue OLEDs were fabricated by using materials **1–3** as the dopant in the emitting layers. A device using 4,4′-[1,6-Pyrenediylbis(9,10-dimethylfluoren-2-yl-amino)]bis-benzonitrile (**3**) showed highly efficient blue emission with the luminous efficiency of 8.94 cd/A, power efficiency of 4.40 lm/W, external quantum efficiency of 6.62% at 20 mA/cm^2, and the CIE coordinates of (0.16, 0.23) at 6.0 V, respectively. This study indicates that OLED devices using diarylamine-substituted pyrene derivatives as blue dopants exhibit the outstanding performances.

Acknowledgment: This research was supported by Samsung Display and the MSIP (Ministry of Science, ICT and Future Planning), Korea, under the ITRC(Information Technology Research Center) support program (IITP-2017-2012-0-00542) supervised by the IITP (Institute for Information and communications Technology Promotion).

References and Notes

1. J. Lewis, S. Grego, B. Chalamala, E. Vick, and D. Temple, *Appl. Phys. Lett.* 85, 3450 (**2004**).
2. S. Kim, H. Kwon, S. Lee, H. Shim, Y. Chun, W. Choi, J. Kwack, D. Han, M. Song, S. Kim, S. Mohammadi, I. Kee, and S. Y. Lee, *Adv. Mater.* 23, 3511 (**2011**).
3. I. Moraes, S. Scholz, M. Hermenau, M. L. Tietze, T. Schwab, S. Hofmann, and M. C. Gather, K. Leo, *Organic Electronics* 26, 158 (**2005**).
4. X. Yang, X. Xu, and G. Zhou, *J. Mater. Chem. C* 3, 913 (**2015**).
5. M. Zhu and C. Yang, *Chem. Soc. Rev.* 42, 4963 (**2013**).
6. H. Shin, C. Lin, H. Shin, and C. Cheng, *Adv. Mater.* 19, 1409 (**2002**).
7. S. Tang, W. Li, F. Shen, D. Liu, B. Yang, and Y. Ma, *J. Mater. Chem.* 22, 4401 (**2012**).
8. Z. Wanga, C. Xu, W. Wang, X. Dong, B. Zhao, and B. Ji, *Dyes and Pigments* 92, 732 (**2012**).
9. S. Jeong, S. Park, K. Kim, Y. Kwon, K. Ha, B. Choi, and Y. Han, *J. Nanosci. Nanotechnol.* 11, 4351 (**2011**).
10. D. Chercka, S. Yoo, M. Baumgarten, J. Kim, and K. Müllen, *J. Mater. Chem. C* 2, 9083 (**2014**).
11. H. Fukagawa, T. Shimizu, N. Ohbe, S. Tokito, K. Tokumaru, and H. Fujikake, *Org. Electron.* 13, 1197 (**2012**).
12. W. Jia, T. M. Cormick, Q. Liu, H. Fukutani, M. Motala, R. Wang, Y. Tao, and S. Wang, *J. Mater. Chem.* 14, 3344 (**2004**).
13. S. Ku, L. Chi, W. Hung, S. Yang, T. Tsai, K. Wong, Y. Chenc, and C. Wu, *J. Mater. Chem.* 19, 1 (**2009**).
14. Z. Liang, Y. Li, J. Yang, Y. Ren, and X. Tao, *Tetrahedron Letters* 52, 1329 (**2011**).
15. J. Huang, N. Sun, Y. Dong, R. Tang, P. Lu, P. Cai, Q. Li, D. Ma, J. Qin, and Z. Li, *Adv. Funct. Mater.* 23, 2329 (**2013**).
16. Z. Zhao, S. Chen, J. Lam, Z. Wang, P. Lu, F. Mahtab, H. Sung, I. Williams, Y. Ma, H. Kwok, and B. Tang, *J. Mater. Chem.* 21, 7210 (**2011**).

Received: 27 November 2017. Accepted: 22 February 2018.